Mismatches in the Influenza A Virus RNA Panhandle Prevent Retinoic Acid-Inducible Gene I (RIG-I) Sensing by Impairing RNA/RIG-I Complex Formation

Stéphanie Anchisi, Jessica Guerra, Geneviève Mottet-Osman, ⓘ Dominique Garcin

Department of Microbiology and Molecular Medicine, Faculty of Medicine, University of Geneva, Geneva, Switzerland

Influenza virus RNA (vRNA) promoter panhandle structures are believed to be sensed by retinoic acid-inducible gene I (RIG-I). The occurrence of mismatches in this double-stranded RNA structure raises questions about their effect on innate sensing. Our results suggest that mismatches in vRNA promoters decrease binding to RIG-I *in vivo*, affecting RNA/RIG-I complex formation and preventing RIG-I activation. These results can be inferred to apply to other viruses and suggest that mismatches may represent a general viral strategy to escape RIG-I sensing.

Detection of viral infections at the cellular level is crucial for the establishment of an innate immune response. Accordingly, viruses have developed strategies to circumvent this response. They can actively block the pathways involved or prevent the formation of viral molecular patterns sensed by specific cellular receptors, such as retinoic acid-inducible gene I (RIG-I) and melanoma differentiation-associated protein 5, that recognize viral RNA patterns. For RIG-I, this pattern consists of double-stranded RNA (dsRNA) structures of various lengths, with 5′ tri- or diphosphate (5′ ppp or 5′ pp, respectively) base-paired ribonucleotides (1, 2). For segmented negative-strand RNA viruses, dsRNA structures are found in panhandles formed by base pairing of conserved and complementary 5′ and 3′ genome ends, which activate RIG-I
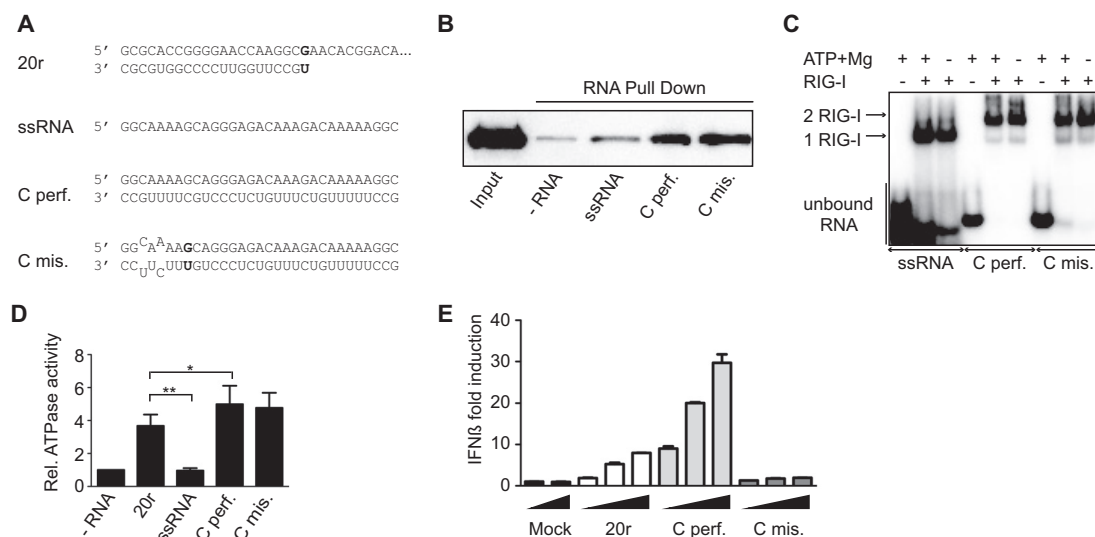
FIG 1 Mismatches do not affect RIG-I binding and ATPase activity but prevent IFN-β activation. (A) Sequences of the RNAs used to mimic the influenza virus cRNA panhandle structures with (mis.) or without (perf.) mismatches. (B) RIG-I binding. RNA pulldown assays were performed with 13 pmol of biotinylated RNA ligands (as previously described [12]) and 13 pmol of His–RIG-I (16). Reaction products were analyzed by Western blotting with antihistidine antibody (1:2,000, H1029; Sigma). (C) RIG-I oligomerization was monitored by EMSA. Radiolabeled RNAs (25 pmol) were incubated with purified His–RIG-I (50 pmol of RIG-I). Reaction products were analyzed on native gradient acrylamide gel and revealed by phosphorimaging (Typhoon; GE Healthcare Life Sciences) (12). (D) Relative (Rel.) RIG-I ATPase activity. Purified RIG-I was incubated at 37°C with [γ-³²P]ATP in the presence of various RNA ligands as indicated. Data are presented as the mean ± the standard error of the mean (*n* = 4). Statistical significance: NS, $P > 0.05$; *, $0.01 \leq P < 0.05$; **, $P < 0.001$ (12). (E) IFN-β promoter activation. A549 cells were transfected with luciferase-based reporter gene plasmids (pβ-IFN-fl-lucter, which carries the firefly luciferase gene driven by the human IFN-β promoter [17], and pTK-rl-lucter, which carries the *Renilla* luciferase-encoding gene [Promega] driven by the herpes simplex virus thymidine kinase promoter) and increasing amounts (200, 400, and 800 ng) of the RNAs indicated. Relative luciferase activation (fold IFN-β induction) was calculated by normalization to the mock-treated control and is represented as the mean ± the standard deviation (*n* = 2) (12).

(3, 4). To avoid detection, viruses have evolved strategies to prevent their formation. Some arenaviruses and bunyaviruses have unusual ways to initiate genome replication, leading to the formation of panhandles with a non-base-paired 5′ pppN overhang or with a 5′ monophosphate end, respectively (5–7). These structures did not activate RIG-I (7, 8) and, in the case of arenaviruses, were seen as a viral decoy strategy to prevent RIG-I activation from *bona fide* ligands (9).

Influenza virus genome promoters are contained within their mostly complementary genome ends, which can form 5′ ppp blunt-ended dsRNAs with conserved mismatches (see Fig. 1A and 3A). When these promoter sequences are bound to their polymerase, the complementary genome ends cannot form dsRNA, except for a region relatively distant from the 5′ ppp and 3′ OH ends (10, 11). However, a fraction of the influenza virus genome promoters is likely not bound to the polymerase during infection. As residues close to the 5′ ppp blunt end of RNA duplexes are critical for RIG-I ATPase activity (12), the presence of mismatches in influenza virus panhandles raises the possibility that, in addition to their primary role in RNA synthesis, mismatches represent a viral strategy to minimize detection by RIG-I.

To study the effect of these mismatches on RIG-I activation, we designed synthetic dsRNAs based on the H1N1 Taiwan NS segment that mimic the influenza virus panhandles, with or without mismatches (see Fig. 1A and 3A). To obtain a 5′ ppp RNA, the top strand was made *in vitro* by using a T7 polymerase. For this purpose, the initial AG nucleotides were changed to GG. The length of these panhandle-like structures was extended to 30 bp (see Fig. 1, 2, and 4) to circumvent stability problems and to monitor only the effects of the mismatches. The 5′ ppp RNA made *in vitro* was used as a single-stranded RNA (ssRNA) control, and a dsRNA of 20 bp (20r) known to activate RIG-I was used as a positive control (Fig. 1A). We first studied the binding of these dsRNAs to RIG-I. Pulldown experiments showed that RIG-I binds equally to dsRNAs mimicking influenza virus cRNA panhandle structures with (Cmis.) or without (Cperf.) mismatches (Fig. 1B). Using a different approach, Liu et al. have shown recently that the panhandle structure without mismatches exhibited higher affinities for RIG-I (3). In addition, the presence of mismatches did not influence the ability of RIG-I to form dimers (2 RIG-I) on these dsRNAs, as shown by electrophoretic mobility shift assays (EMSA) (Fig. 1C, Cperf. and Cmis. versus ssRNA). In EMSA, addition of ATP and MgCl₂, which allows RIG-I ATPase activity, had no effect on RIG-I dimerization, as previously observed (12). Interestingly, although these mismatches are positioned in key residues for RIG-I ATPase activity (12), their presence had no effect on RIG-I ATPase activity *in vitro*, which was higher than that of 20r because of their greater dsRNA length (30 versus 20 bp) (Fig. 1D). Nevertheless, when these dsRNAs were tested for the ability to activate the beta interferon (IFN-β) promoter in a luciferase-based reporter gene assay, the presence of mismatches completely abrogated activation (Fig. 1E). Here again, Cperf. was more active than 20r, very likely because of its greater dsRNA length. To rule out the hypothesis of selective RNA degradation, A549 cells engineered to express the green fluorescent protein (GFP)-encoding gene under the control of the IFN-β promoter (13) were transfected with dsRNAs labeled with Cy5-fluorescent CTP. The cells were then analyzed by flow cytometry for GFP expression (IFN-β activation) and Cy5 fluorescence (RNA stability) at 9 and 24 h post-transfection. The results confirmed that, contrary to Cperf., Cmis.
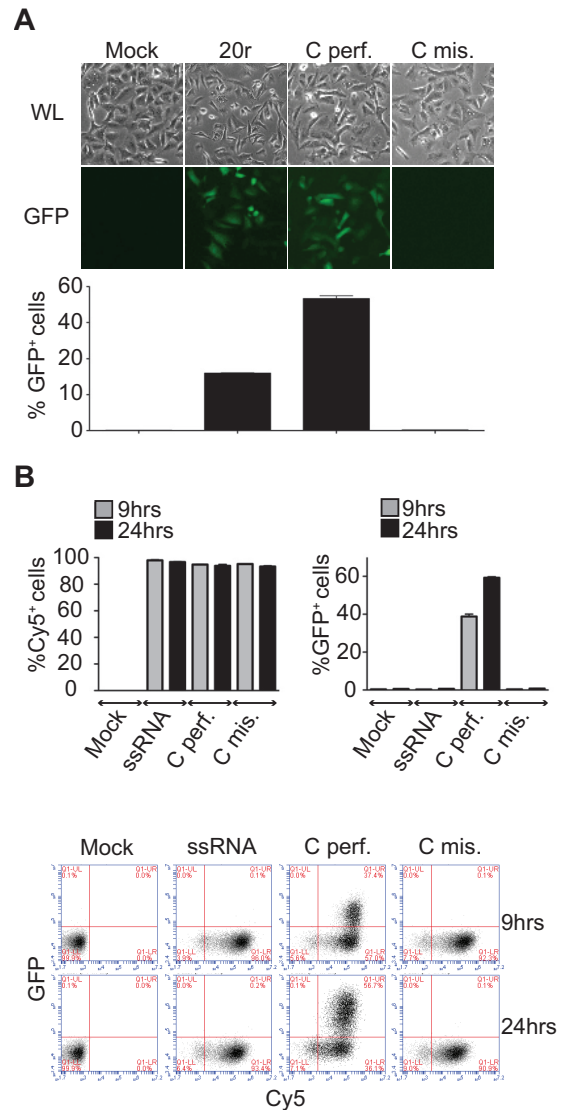

FIG 2 Mismatches do not affect RNA stability. (A, B) IFN-β promoter activation. A549/pr(IFN-β).GFP reporter cells (13) were transfected with 400 ng of the RNAs indicated for 24 h before fluorescence-activated cell sorter (FACS) analysis. (A) At the top are white light (WL) and fluorescence (GFP) microscope pictures. At the bottom are flow cytometry data. Results are plotted as percentages of GFP-positive cells (x axis). Data are presented as means ± standard deviations (n = 2). (B) RNA stability. A549/pr(IFN-β).GFP reporter cells were transfected with Cy5-labeled RNAs, and Cy5 fluorescence was monitored over time by FACS analysis. Results are plotted as percentages of Cy5- or GFP-positive cells. Data are presented as means ± standard deviations (n = 2). At the bottom are representative plots of the FACS data. Results are plotted as percentages of Cy5 (x axis)- and GFP (y axis)-positive cells.

did not induce IFN-β under conditions where no difference in Cy5 fluorescence could be detected (Fig. 2A and B), ruling out RNA degradation as an explanation for the lack of IFN induction.

We further tested the effects of individual mismatches (Fig. 3A, Cmis.3 and Cmis.5). As shown in Fig. 1D for the double-mismatch construct (Cmis.), the two single-mismatch dsRNAs induced RIG-I ATPase as efficiently as the perfect dsRNA (Fig. 3B). When tested for the ability to induce the IFN-β promoter in a reporter gene assay, the duplex with the mismatch at position 3 (Cmis.3) exhibited no stimulatory activity, while Cmis.5 retained some stimulatory activity (Fig. 3C, black bars). We have previ-
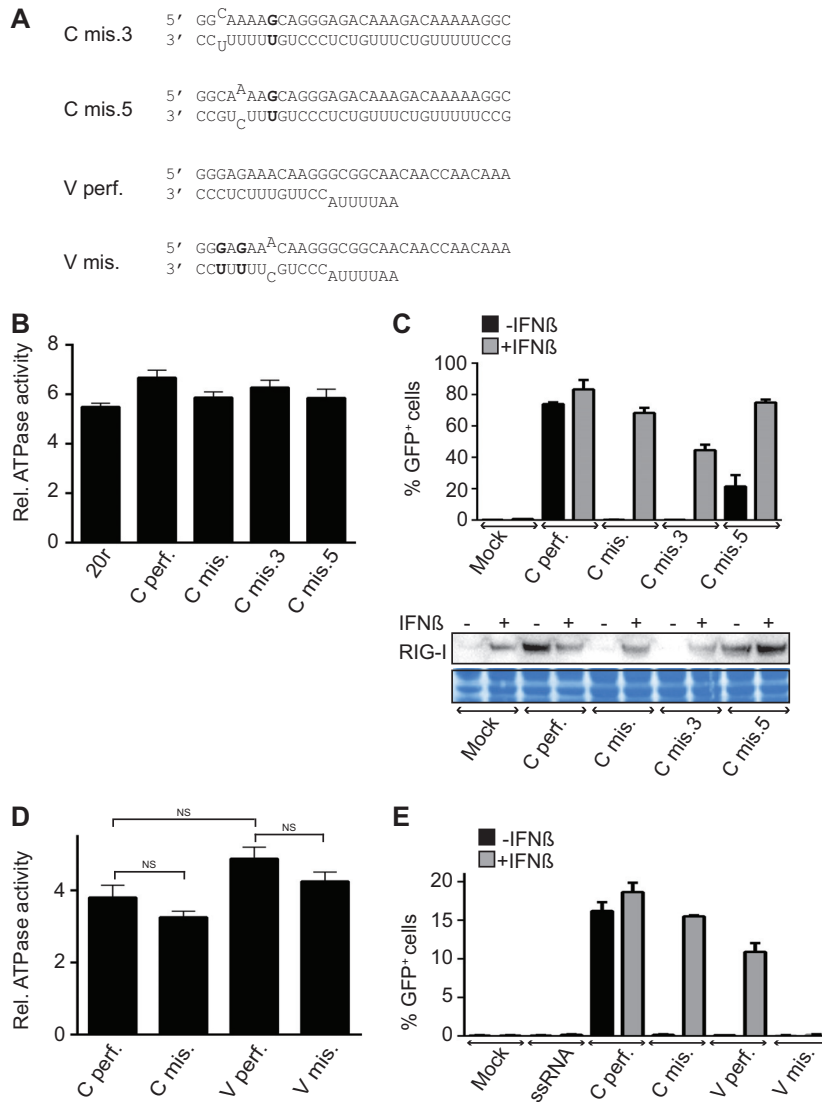
FIG 3 A single mismatch on dsRNA is enough to limit IFN-β induction. (A) Sequences of the RNAs used. (B) RIG-I ATPase activity. Purified RIG-I was incubated at 37°C with [γ-^{32}P]ATP in the presence of various RNA ligands as indicated. Data are presented as the mean ± the standard error of the mean ($n = 4$). Statistical significance: NS, $P > 0.05$; *, $0.01 \leq P < 0.05$; **, $P < 0.001$ (12). (C) IFN-β promoter activation. A549/pr(IFN-β).GFP reporter cells were transfected with 500 ng of the RNAs indicated for 24 h with or without IFN-β treatment 6 h prior to transfection. At the top are the percentages of GFP-positive cells measured by FACS analysis. Data are presented as the mean ± the standard deviation ($n = 2$). At the bottom are the intracellular levels of RIG-I analyzed by Western blotting. As a loading control, the membrane was stained with Coomassie blue after immunoblotting. (D) RNA-induced ATPase activity of RIG-I. Purified RIG-I was incubated at room temperature with [γ-^{32}P]ATP in the presence of various RNA ligands as indicated. Data are presented as the mean ± the standard error of the mean ($n = 5$). Statistical significance: NS, $P > 0.05$; **, $P < 0.001$. (E) IFN-β promoter activation. A549/pr(IFN-β).GFP reporter cells were transfected with 500 ng of the RNAs indicated for 24 h with or without IFN-β treatment 6 h prior to transfection. Results are plotted as the percentages of GFP-positive cells measured by flow cytometry. Data are presented as the mean ± the standard deviation ($n = 2$).

ously shown that IFN-β promoter activation can be enhanced by pretreating cells (priming) with IFN-β (12). Under these conditions, the inactive dsRNAs with single or double mismatches now activated the IFN-β promoter, confirming that these RNAs are not degraded (Fig. 3C, gray bars). The observed increased RIG-I levels upon priming (Fig. 3C) could promote the formation of an active tetrameric RIG-I complex (14), especially for unstable RNA/RIG-I complexes, as seen for dsRNAs shorter than 13 bp (12). When short dsRNAs mimicking the precise length of influenza vRNA panhandles (13 bp) with or without mismatches, G-U bonds, and an AU tail mimicking the loop were used (Fig. 3A, Vperf. and Vmis.), similar results in ATPase activity and RIG-I activation in cells and primed

cells were obtained, with the exception of Vmis., which remained inactive even in IFN-primed cells (Fig. 3D and E). Taken together, these results suggested that these mismatches might act by lowering the formation of the RNA/RIG-I complex.

To monitor the formation of the RNA/RIG-I complex, we performed *in vivo* RNA pulldown experiments after transfection of biotinylated dsRNAs in cells overexpressing RIG-I. Results presented in Fig. 4A show that significantly less RIG-I was found associated with dsRNAs with mismatches than with perfect dsRNAs (65% versus 100%, Fig. 4A). In order to further test this complex formation *in vitro*, competition assays were performed in RNA pulldown experiments using an excess of nonbiotinylated
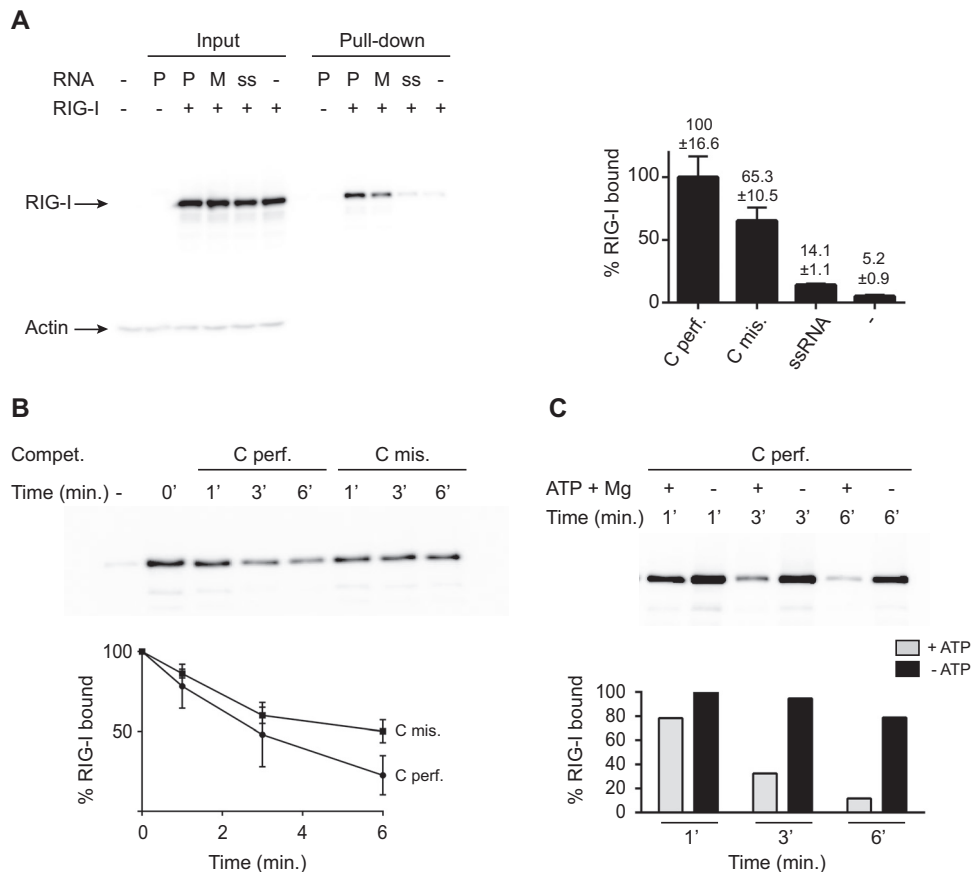
FIG 4 Mismatches destabilize RNA/RIG-I complex formation. (A) *In vivo* RIG-I binding. 293T cells were first transfected with pEF-Bos-RIG-I (2 μg) for 24 h and then transfected with 2 μg of biotinylated perfect cRNA (Cperf.) or mismatch RNA (Cmis.). As a control, cells were transfected with 2 μg of biotinylated ssRNA. At 2 h after RNA transfection, cells were lysed and lysates were incubated with streptavidin beads for 2 h at 4°C to pull down RNA-bound RIG-I. Reactions were analyzed by Western blotting with anti-RIG-I antibody (ALX-804-849-C100; Enzo Life Sciences). Data are presented as the mean ± the standard deviation ($n = 2$). (B) Competition (Compet.) in an RNA pulldown assay. Thirteen picomoles of biotinylated perfect cRNA was bound to streptavidin beads by incubation for 2 h at 4°C. Thirteen picomoles of His–RIG-I protein was added to the reaction mixtures for 15 min of incubation at 37°C. A competition assay was performed with a 3-fold excess of either nonbiotinylated perfect (Cperf.) or mismatched (Cmis.) cRNA for 1, 3, or 6 min at 37°C in the presence of ATP and MgCl$_2$. RIG-I binding was monitored by Western blotting and quantified with anti-RIG-I antibody. After quantification, results were plotted as the percentage of RIG-I that remained bound to the beads as a function of time. Data are presented as the mean ± the standard deviation ($n = 5$). (C) Competition in an RNA pulldown assay. Thirteen picomoles of biotinylated perfect cRNA was bound to streptavidin beads by incubation for 2 h at 4°C. Thirteen picomoles of His–RIG-I protein was added to the reaction mixtures for 15 min of incubation at 37°C. A competition assay was performed with a 3-fold excess of either nonbiotinylated perfect cRNA (Cperf.) for 1, 3, or 6 min at 37°C in the absence or presence of ATP and MgCl$_2$ as indicated. RIG-I binding was monitored by Western blotting and quantified with anti-RIG-I antibody. A representative experiment is shown. Western blot quantifications were performed with ImageJ version 1.44p (National Institutes of Health, Bethesda, MD; http://imagej.nih.gov/ij/).

dsRNAs with (Cmis.) or without (Cperf.) mismatches under conditions where RIG-I ATPase activity and related RNA recycling are allowed (12). Figure 4B shows that more RIG-I is associated with the biotinylated RNA when the competitor has mismatches. This indicates that the rate of RIG-I exchange is lower with a competitor carrying mismatches (50% versus 22% after 6 min of incubation), consistent with lower stability of the RNA/RIG-I complex in this case. As shown in Fig. 4C, the rate of RIG-I exchange and related RNA/RIG-I complex stability is dependent on RIG-I ATPase activity since no exchange is observed in the absence of ATP and MgCl$_2$. In conclusion, mismatches as found in the panhandle structures of segmented negative-strand RNA viruses may prevent RIG-I activation by impairing the formation of stable RNA/RIG-I complexes. As mismatches can be observed in the panhandle structure of other segmented negative-strand viruses (15), the results presented here can be inferred to apply to other viruses and suggest that mismatches could represent a general viral strategy to escape RIG-I sensing.

REFERENCES

1. **Schlee M.** 2013. Master sensors of pathogenic RNA—RIG-I like receptors. Immunobiology **218:**1322–1335. http://dx.doi.org/10.1016/j.imbio.2013.06.007.
2. **Goubau D, Schlee M, Deddouche S, Pruijssers AJ, Zillinger T, Goldeck M, Schuberth C, Van der Veen AG, Fujimura T, Rehwinkel J, Iskarpatyoti JA, Barchet W, Ludwig J, Dermody TS, Hartmann G, Reis e Sousa C.** 2014. Antiviral immunity via RIG-I-mediated recognition of

RNA bearing 5′-diphosphates. Nature **514:**372–375. http://dx.doi.org/10.1038/nature13590.

3. **Liu G, Park HS, Pyo HM, Liu Q, Zhou Y.** 2015. Influenza A virus panhandle structure is directly involved in RIG-I activation and interferon induction. J Virol **89:**6067–6079. http://dx.doi.org/10.1128/JVI.00232-15.

4. **Weber M, Gawanbacht A, Habjan M, Rang A, Borner C, Schmidt AM, Veitinger S, Jacob R, Devignot S, Kochs G, Garcia-Sastre A, Weber F.** 2013. Incoming RNA virus nucleocapsids containing a 5′-triphosphorylated genome activate RIG-I and antiviral signaling. Cell Host Microbe **13:**336–346. http://dx.doi.org/10.1016/j.chom.2013.01.012.

5. **Garcin D, Kolakofsky D.** 1992. Tacaribe arenavirus RNA synthesis in vitro is primer dependent and suggests an unusual model for the initiation of genome replication. J Virol **66:**1370–1376.

6. **Garcin D, Lezzi M, Dobbs M, Elliott RM, Schmaljohn C, Kang CY, Kolakofsky D.** 1995. The 5′ ends of Hantaan virus (*Bunyaviridae*) RNAs suggest a prime-and-realign mechanism for the initiation of RNA synthesis. J Virol **69:**5754–5762.

7. **Habjan M, Andersson I, Klingstrom J, Schumann M, Martin A, Zimmermann P, Wagner V, Pichlmair A, Schneider U, Muhlberger E, Mirazimi A, Weber F.** 2008. Processing of genome 5′ termini as a strategy of negative-strand RNA viruses to avoid RIG-I-dependent interferon induction. PLoS One **3:**e2032. http://dx.doi.org/10.1371/journal.pone.0002032.

8. **Marq JB, Kolakofsky D, Garcin D.** 2010. Unpaired 5′ ppp-nucleotides, as found in arenavirus double-stranded RNA panhandles, are not recognized by RIG-I. J Biol Chem **285:**18208–18216. http://dx.doi.org/10.1074/jbc.M109.089425.

9. **Marq JB, Hausmann S, Veillard N, Kolakofsky D, Garcin D.** 2011. Short double-stranded RNAs with an overhanging 5′ ppp-nucleotide, as found in arenavirus genomes, act as RIG-I decoys. J Biol Chem **286:**6108–6116. http://dx.doi.org/10.1074/jbc.M110.186262.

10. **Chang S, Sun D, Liang H, Wang J, Li J, Guo L, Wang X, Guan C, Boruah BM, Yuan L, Feng F, Yang M, Wang L, Wang Y, Wojdyla J, Li L, Wang J, Wang M, Cheng G, Wang HW, Liu Y.** 2015. Cryo-EM structure of influenza virus RNA polymerase complex at 4.3 A resolution. Mol Cell **57:**925–935. http://dx.doi.org/10.1016/j.molcel.2014.12.031.

11. **Pflug A, Guilligay D, Reich S, Cusack S.** 2014. Structure of influenza A polymerase bound to the viral RNA promoter. Nature **516:**355–360. http://dx.doi.org/10.1038/nature14008.

12. **Anchisi S, Guerra J, Garcin D.** 2015. RIG-I ATPase activity and discrimination of self-RNA versus non-self-RNA. mBio **6:**e02349. http://dx.doi.org/10.1128/mBio.02349-14.

13. **Chen S, Short JA, Young DF, Killip MJ, Schneider M, Goodbourn S, Randall RE.** 2010. Heterocellular induction of interferon by negative-sense RNA viruses. Virology **407:**247–255. http://dx.doi.org/10.1016/j.virol.2010.08.008.

14. **Wu B, Peisley A, Tetrault D, Li Z, Egelman EH, Magor KE, Walz T, Penczek PA, Hur S.** 2014. Molecular imprinting as a signal-activation mechanism of the viral RNA sensor RIG-I. Mol Cell **55:**511–523. http://dx.doi.org/10.1016/j.molcel.2014.06.010.

15. **Weber M, Weber F.** 2014. Segmented negative-strand RNA viruses and RIG-I: divide (your genome) and rule. Curr Opin Microbiol **20:**96–102. http://dx.doi.org/10.1016/j.mib.2014.05.002.

16. **Hausmann S, Marq JB, Tapparel C, Kolakofsky D, Garcin D.** 2008. RIG-I and dsRNA-induced IFNbeta activation. PLoS One **3:**e3965. http://dx.doi.org/10.1371/journal.pone.0003965.

17. **King P, Goodbourn S.** 1994. The beta-interferon promoter responds to priming through multiple independent regulatory elements. J Biol Chem **269:**30609–30615.